Optical Diagnostics of a Low Temperature Argon Thruster

IEPC-2011-169

Presented at the 32nd International Electric Propulsion Conference,
Wiesbaden • Germany
September 11 – 15, 2011

K. Katsonis[1] and Ch. Berenguer[2]
Data Evaluation & Diagnostics ALgorithms Of Systems (DEDALOS EPE), Thessaloniki, Hellas

D. Pavarin[3], A. Lucca Fabris[4], F. Trezzolani[5] and M. Faenza[6]
Center of Studies and Activities for Space (CISAS) "G. Colombo", University of Padua, Padua, Italy

P. Tsekeris[7] and S. Cohen[8]
Physics Department, University of Ioannina, GR-45110 Ioannina, Greece

and

M. Cornille[9]
LUTH, CNRS, Observatoire de Paris, 92190 Meudon, France &
Data Evaluation & Diagnostics ALgorithms Of Systems (DEDALOS EPE), Thessaloniki, Hellas

Abstract: We have diagnosed by optical emission spectroscopy a relatively low temperature helicon plasma thruster working with argon in various conditions and configurations, in order to explain and optimize its functioning. This work concerns specifically the helicon plasma thruster developed in the frame of the research project Helicon Plasma Hydrazine Combined Micro (HPH.com).

Nomenclature

A_{ij}	=	transition probability
Ar I, II,..	=	successive spectra of the argon homo-nuclear sequence, Ar^0, Ar^+, Ar^{++}, Ar^{+++}
Ar I,II,III/C-R	=	collisional – radiative model containing Ar I, II and III levels and Ar IV continua
CATS	=	Cowan atomic structure code

[1] Director, DEDALOS EPE, katsonis@dedalos.eu
[2] Project Manager, DEDALOS EPE, berenguer@dedalos.eu
[3] Researcher, Department of Mechanical Engineering, Center of Studies and Activities of Space (CISAS), University of Padua, daniele.pavarin@unipd.it
[4] PhD Student, Center of Studies and Activities of Space (CISAS), University of Padua, andrea.luccafabris@studenti.unipd.it
[5] Junior Engineer, Center of Studies and Activities of Space (CISAS), University of Padua, f.trezzolani@hit09.com
[6] PhD Student, Center of Studies and Activities of Space (CISAS), University of Padua, martina.faenza@studenti.unipd.it
[7] Associate Professor, Department of Physics, tsekeris@uoi.gr
[8] Assistant Professor, Department of Physics, scohen@uoi.gr
[9] Research associate with Paris Observatory & Scientific Director, DEDALOS EPE marguerite.cornille@obspm.fr

CbA = Coulomb approximation code
CISAS = Center of Studies and Activities for Space (CISAS) “G. Colombo”, University of Padua, Padua, Italy
C-R = Collisional-Radiative
DW = distorted wave approximation
DEDALOS = Data Evaluation & Diagnostics ALgorithms Of Systems
FOMBT = first order many body theory
GL = ground level compound, composed by one sole level for Ar I, two for Ar II, five for Ar III and Ar IV
HPH.com = Helicon Plasma Hydrazine Combined Micro project, European consortium, 7th Framework Programme of the EU
IC = Inductively Coupled
IPP = Institute of Plasma Physics, Greifswald
jK/LS = coupling schemes
l = orbital quantum number, *s* = 0, *p* = 1, *d* = 2, *f* = 3, …
LANL = Los Alamos National Laboratory
LPGP = Laboratoire de Physique des Gaz et des Plasmas
LPP = Laboratoire de Physique des Plasmas
LTE = Local Thermodynamic Equilibrium
MW = Micro-Wave
n = principal quantum number, here *n* = 3, 4
n_e = electronic density
NIST = National Institute of Standards and Technology, Gaithersburg (USA)
OES = Optical Emission Spectroscopy
ONERA = Office National d'Etudes et de Recherches Aérospatiales
PIC = Particle in Cell type code
RF = Radio-Frequency
T_e = electronic temperature
SPT-50 = prototype stationary plasma thruster, 50 mm of diameter
SST = SUPERSTRUCTURE code
λ = wavelength
σ_{exc} = electron collision excitation cross section
σ_I = electron collision ionization cross section

I. Introduction

OPTICAL Emission Spectroscopy (OES) constitutes a powerful non-perturbing method of plasma diagnostics, able to give trustful results to be compared with those obtained with other experimental tools, notably the often used plasma probes under their various refinements[1]. However, a first problem hampering the common use of OES is that industrial plasmas are very often outside Local Thermodynamic Equilibrium (LTE). In this very common case, the measured line intensities cannot be used directly to evaluate the electronic density n_e and electronic temperature T_e values in a radiating point. A detailed Collisional-Radiative C-R model[2] becomes necessary in order to calculate the n_e and T_e values corresponding to the measured line intensities, instead of using the equilibrium values. Elaboration of the C-R model calls for an extended set of radiative and collisional data, which are often cumbersome to compile. Moreover, a previous validation of the model is necessary for obtaining trustful results[3]. A second indirect problem comes from the fact that the registered radiation corresponds to a sole point of the plasma under study. With exception of the plasma edge, the radiation is registered only after passing from other plasma regions which may be in different states, typically described by other n_e , T_e sets. Thus, not only distinct points are diagnosed but also the acquired spectra, being possibly somehow distorted, may lead to inaccurate n_e , T_e sets.

Sole acquisition of some n_e , T_e sets is not sufficient for non-homogeneous plasmas study: information on the bulk plasma properties is not directly made available. In order to get a realistic image of the plasma status a model of the plasma, often a “global” one, must be used in conjunction with the measured line intensities and any other experimental results available. In describing one helicon plasma thruster, we had used previously a simplified global model incorporating a minimum of atomic constants[4, 5] and also a detailed Particle in Cell (PIC) one. Parameters from the global model were compared with those obtained by the PIC model calculations. Keep in mind that in formulating global models, attributing a separate temperature to each of the plasma constituents reflects the non-LTE status of the plasma. Moreover, for non-equilibrium plasmas, even the electron distribution function, which is in the basis of the temperature definition, may be non-Maxwellian[6]. Occasionally, the quasi-neutrality assumption may also be not valid. Inclusion in a global model of such atomic details as excited level populations allows for a direct comparison of the experimental results with the theoretical ones. Separate consideration of the emission lines from species in a different ionization stage encountered in various plasma regions is essential for the diagnostics refinement, as described later in section IV. Thus, a global model allows for comparison of the detailed "zero dimensional" C-R model values with the approximate values describing the bulk of the plasma.

Systematic optical diagnostics developed previously[7] is used here in obtaining a trustful evaluation of n_e and T_e at various points of a helicon thruster device, relying on the emission spectroscopy of the Ar I, II and III species present in the plasma. Overall description of this experiment located at CISAS Laboratory, is presented in this Conference as a separate contribution[8]. Similar OES tools have been used previously in diagnosing propulsion plasma devices: a SPT-50 thruster made available from the LPP Laboratory of the Polytechnic School[9] and a FEEP Indium micro-thruster which was available at the Onera Laboratory in Palaiseau[10]. Because of the relatively low T_e expected in the HPH.com project thruster, a simple coronal model suggests that taking into consideration only the neutral Ar I, the first two ionization stages Ar II and III and their excited states including ionization continua, should be sufficient for both diagnostics and modeling. The obtained spectra justify this choice *a posteriori,* as we see in section IV.

In general, OES has been often used for diagnostics of various types of plasmas, as micro-wave[11] (MW), radio-frequency[12] (RF) and inductively coupled[13] (IC) plasmas. Specifically, while developing OES diagnostics we analyzed various experimental Ar spectra, a process which contributed to insure validation of our Ar I,II,III/C-R model. Among the most recently studied were spectra from a hollow cathode lamp available in the University of Ioannina[14] and those registered in the DIVA reactor, in a Cu-Magnetron and in a capillary tube, experimental set-ups which are all available in the LPGP Laboratory at Orsay. Also, spectra from the WEGA stellarator of the IPP of Greifswald[15] and from an Ar-Nb lamp at Riga were studied. Experiments which have been previously performed in LPGP and IPP have been described in ref. **16**, where the obtained results were compared and discussed. Moreover, a global model taking account separately of the 4*s* and 4*p* configurations of Ar I has been developed lately, aiming to support OES diagnostics of arc-jet Ar plasmas[17]. The latter can also be used for propulsion devices functioning at higher energies.

In our plasma description, detailed electrons and chemical species (atoms and molecules, both neutral and ionized) are explicitly addressed. A local plasma neutrality condition including all the charged species is assumed throughout. Consequently, the electronic density n_e follows typically the quasi-neutrality approximation expressed here as

$$n_e = n_{Ar+} + 2n_{Ar++} + 3n_{Ar++++} \quad (1)$$

if presence of Ar species up to the three times ionized ground levels is taken into account. Using a C-R model, the expected populations of Ar I, II and III excited states are calculated from the plasma density for any n_e, T_e couple, taking into consideration a set of processes (mainly electron collision ionization and excitation and the inverse recombination and de-excitation processes). Population of an averaged Ar^{+++} GL is also calculated.

Numerous atomic data including structure, transition probabilities, and cross sections of excitation σ_{exc} and ionization σ_I were calculated and evaluated using various methods and codes[18]. Some typical examples are given in a separate contribution presented in this Conference[19].

II. Acquisition of the relevant Ar spectra

Precise spectra in the whole plasma spectral region from the near IR (where persistent Ar I lines are present) to the near UV (where the non-resonant part of the Ar II and Ar III lines appear) are mandatory for satisfactory optical plasma diagnostics of the thruster. The bulk of the Ar I and II lines are situated in the visible region. With increasing ionization stage, the radiation is shifted to shorter wavelengths. Note that the resonant lines which belong to the VUV region, are also very important. Hence, they were the subject of a separate study[19]. The apparatuses to be used for spectral acquisitions must have the necessary resolution, allowing for properly separate and identify the big amount of lines contained in the Ar I, II and III spectra. This is especially important in the wavelength region from 400 nm to 500 nm where intense Ar I and Ar II lines are overlapping and also in the region from 200 nm to 400 nm, where Ar III lines can be easily identified whenever the temperature is high enough. For the optical diagnostics of the helicon thruster we used two Ocean Optics spectrometers: i) an HR4000 with a 25 μm slit and a rather low resolution (about 0.54 nm) going from 380 to 830 nm and ii) an HR4000 with a 5 μm slit and a resolution of about 0.23 nm going from 650 nm down to 200 nm. The spectrometers were employed in combination with 2 m long optical fibers with 0.6 mm core diameter. The heads of the optical fibers were displaced in a fixed position located 5 mm upstream the thruster outlet.

The two spectrometers were used in conjunction, in order to obtain both a global view of the spectrum and also precise information from the lower wavelength region. Line intensities belonging to the main multiplets of Ar I, II and III lines were analyzed and compared with those of the theoretical spectra calculated by our Collisional-Radiative (C-R) model of Ar I,II,III/C-R, see ref. **18**. This comparison allows for determination of the plasma parameters, namely the electronic temperature and electronic density in the emitting plasma region. Measured line intensities were also compared with those from spectra obtained previously in other devices, and notably with those of experimental Ar I, II and III species used here as a benchmark in comparisons with the helicon thruster spectra[14]. These were lately extended with acquisition of two more spectra of neutral and ionized Ar species, obtained by a well-known Fe hollow cathode lamp[20] with a low (2 mA) and a high (10 mA) current. They span an extended wavelength region from 190 nm to 940 nm. Background correction and wavelength calibration have been made, and the grating efficiency has been taken into consideration. No optical fiber was used to avoid any absorption effects.

III. General description of the studied spectra

We proceeded to various Ar spectroscopic measurements which were analyzed on the basis of a C-R model encompassing atomic data calculated and evaluated as described elsewhere[14]. Among the numerous emission spectra which have been registered in the helicon thruster we select here some typical cases belonging to:

i) a wide spectral region from 380 nm to 830 nm and

ii) the short wavelength region of 200 nm to 650 nm.

These spectra concern the main multiplet 4*s* – 4*p* lines of the Ar I ("red" lines), II and III species and other important multiplets expected in the thruster plasma. Background correction of the obtained intensities has been made and also the grating efficiency was taken under consideration. We present an overview of the thruster spectrum in Fig. 1. It shows the main lines of Ar I and Ar II in the wavelength region from 290 nm to 650 nm. Some Ar III lines are also identified in the region 320 to 350 nm, delimited by an ellipse in Fig. 1, as they are not clearly visible. The lines are separated for Ar I and II, according to each species and multiplet. The most intense lines belong to the Ar II 4*s*-4*p* multiplet (shown in red), in the region from about 430 nm to 500 nm. In the present n_e, T_e conditions, these lines are here by far the most intense, prevailing over the well-known Ar I 4*s*-5*p* "blue" lines, appearing in the region from 400 nm to 450 nm, shown in blue. The latter are the main lines of the neutral argon spectrum after the "red" ones,

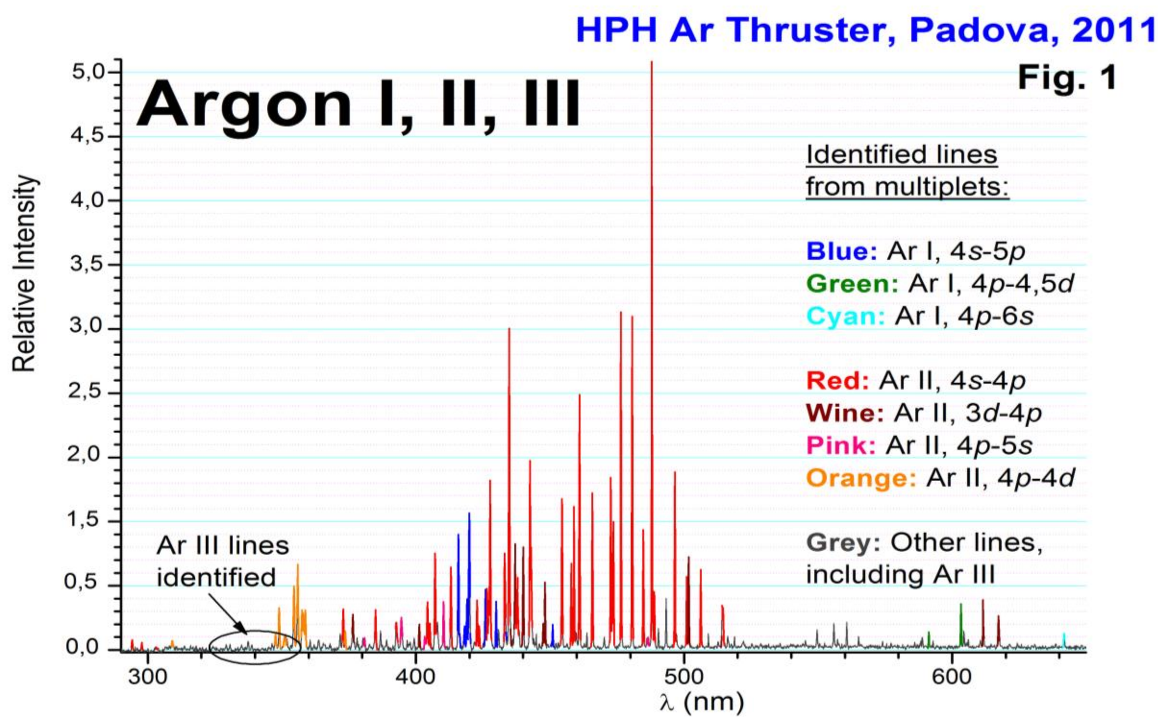

Figure 1. Overview of the thruster Ar spectrum in the wavelength region from 290 to 650 nm. *The main lines of Ar I and Ar II have been identified separately for each multiplet and are marked with different colors.*

which belong roughly to the 700 nm - 900 nm spectral region. Ar I 4*s*-4*p* lines are not shown here, as they are outside the wavelength limits of Fig. 1.

Figures 2, 4, 6, 8 and 10 show the low (2 mA) and high (10 mA) current spectra acquired in the cathode lamp. In these figures, lines belonging to the high current spectra are displaced *ad hoc* slightly to the right (3 nm for Fig. 3 and 0.5 nm for the others) in order to allow for an easy comparison of the intensities belonging to the two different currents. Figures 3, 5, 7, 9 and 11 show the thruster spectra in the same regions. Low/high intensities comparison shows that the cathode plasma was typically near equilibrium. Comparing the spectra from the hollow cathode with those acquired from the thruster indicates that the latter were mostly far from equilibrium.

Our C-R model allows for distinct evaluation of n_e and T_e for each of the Ar I, II and III species present, depending from the spectral acquisition region and, noteworthy, with a higher and a lower intensity magnetic field. In the hotter plasma region expected on the main thruster axis, our emission diagnostics results to T_e of up to 2.5 eV for the lower magnetic field and up to 4.5 eV for the higher, for n_e of about $(1.0 – 4.0)\cdot10^{12}$ cm^{-3}. This is conformal with results from other diagnostic methods. It also corroborates experimental results obtained by other methods including probes, reported for low energy helicon devices. Lately, n_e up to $2.0\cdot10^{11}$ cm^{-3} for low magnetic fields and up to $3.5\cdot10^{11}$ cm^{-3} for higher ones, have been obtained[21]. Besides, measurements of bulk T_e suggested values[22] exceeding 6 eV.

Line intensity measurement of numerous identified lines allowed to obtain experimental A_{ij} values for the main Ar I, II and III multiplets. We compared the experimental results and particularly A_{ij} values coming from the intensity ratio fractions observed in the two current intensities in the hollow cathode, to those of the thruster spectra and to A_{ij} values obtained by using our CbA code[23] based on the Coulomb approximation and to theoretical results obtained previously with the SST[24] and the CATS codes[25]. We occasionally compare our A_{ij} with those evaluated by NIST[26] and with those available in the literature, both theoretical and experimental.

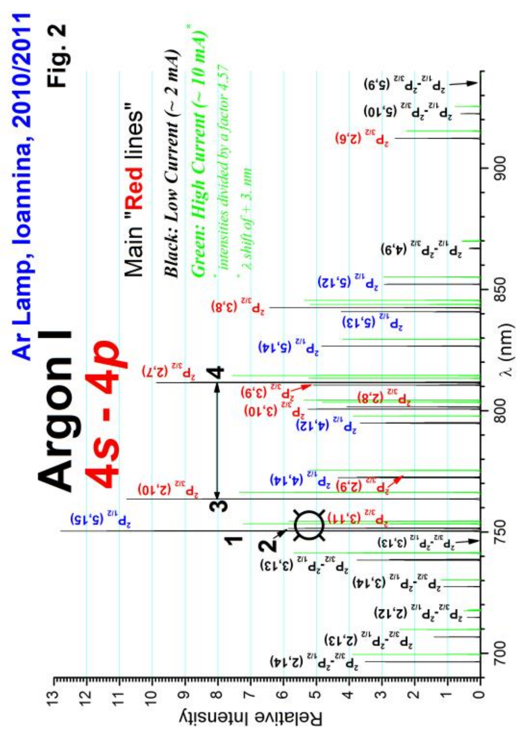

Figure 2. Experimental spectra of the Fe-Ar hollow cathode, Ar I 4*s*-4*p* lines identified.

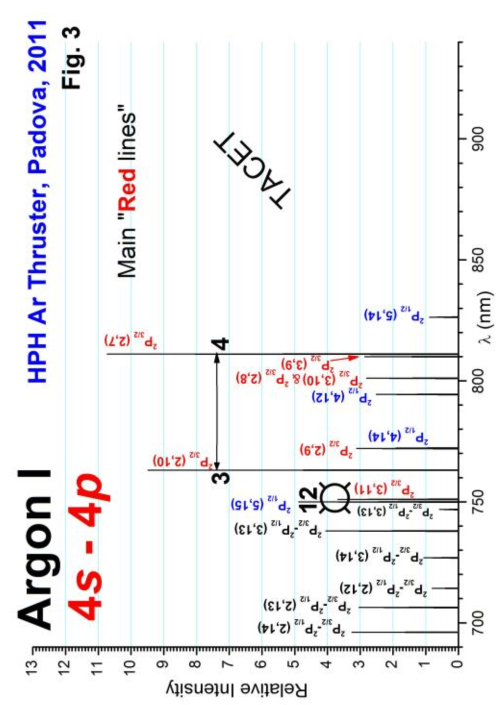

Figure 3. Experimental spectrum of the Ar thruster, Ar I 4*s*-4*p* lines identified.

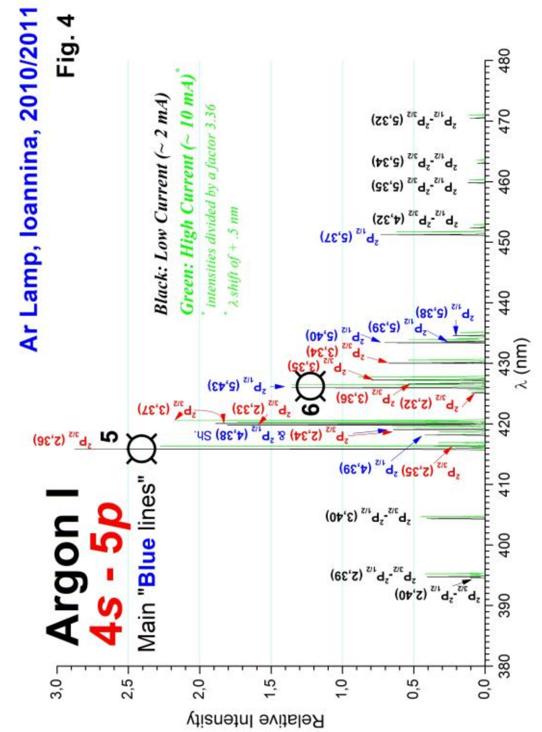

Figure 4. Experimental spectra of the Fe-Ar hollow cathode, Ar I 4*s*-5*p* lines identified.

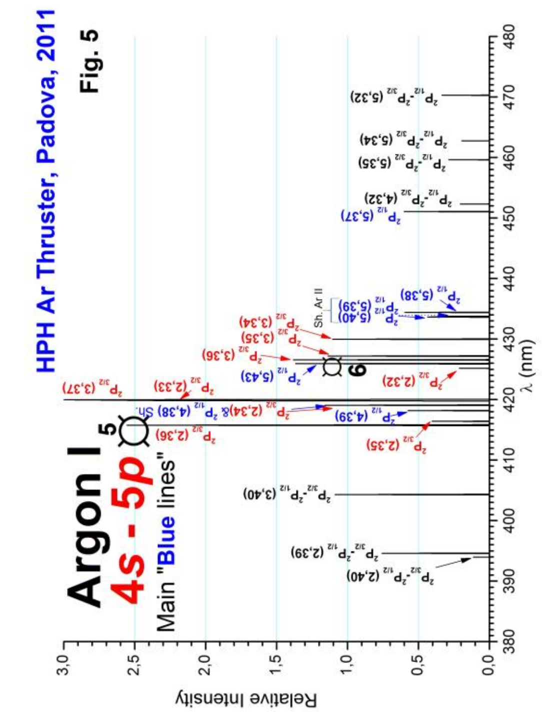

Figure 5. Experimental spectrum of the Ar thruster, Ar I 4*s*-5*p* lines identified.

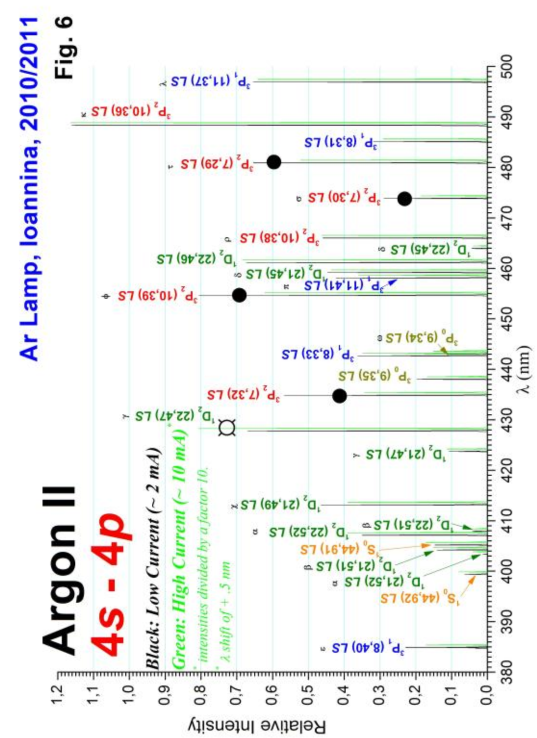

Figure 6. Experimental spectra of the Fe-Ar hollow cathode, Ar II 4*s*-4*p* lines identified.

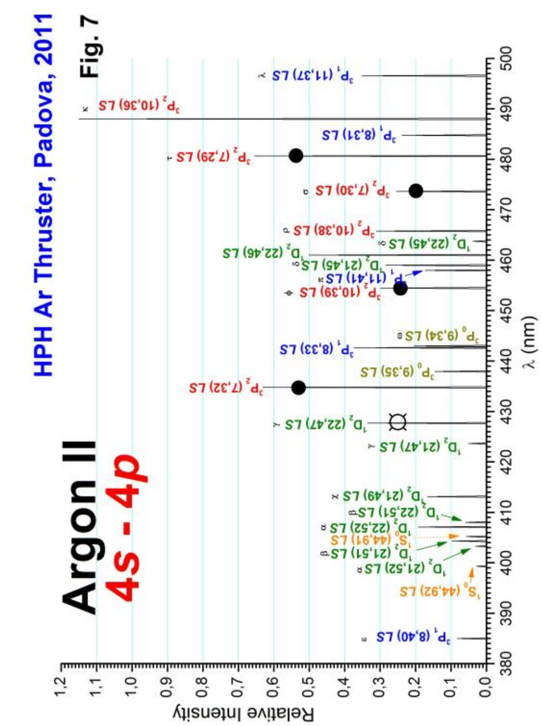

Figure 7. Experimental spectrum of the Ar thruster, Ar II 4*s*-4*p* lines identified.

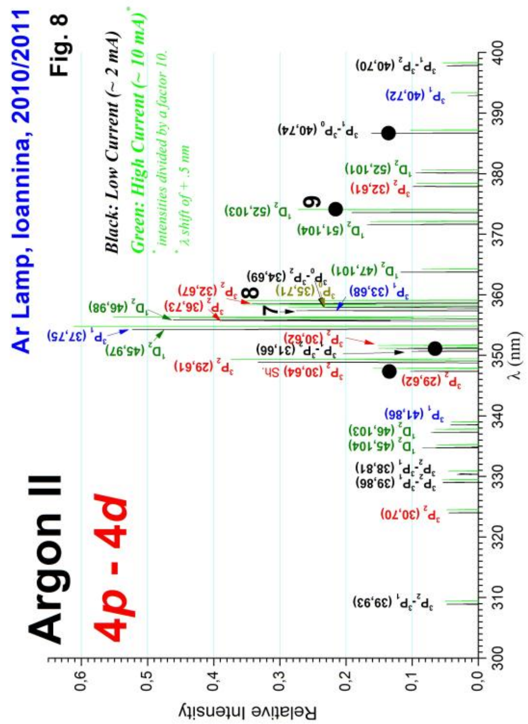

Figure 8. Experimental spectra of the Fe-Ar hollow cathode, Ar II 4*p*-4*d* lines identified.

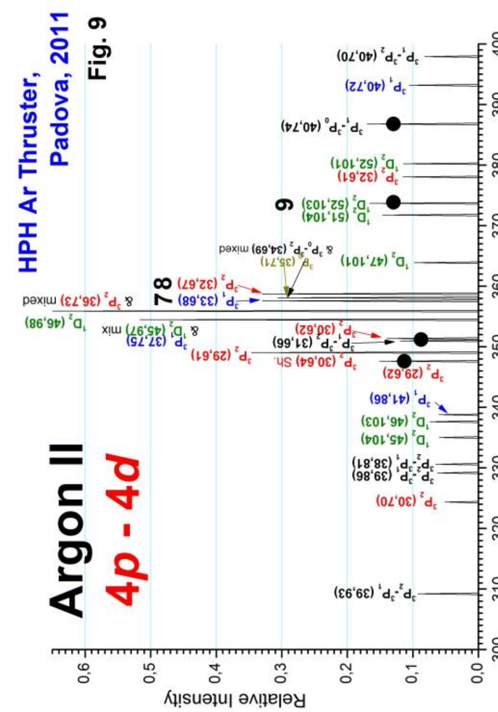

Figure 9. Experimental spectrum of the Ar thruster, Ar II 4*p*-4*d* lines identified.

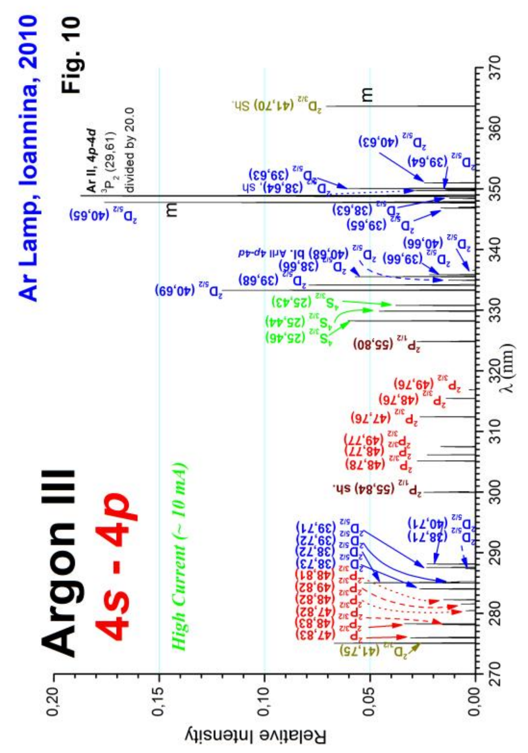

Figure 10. Experimental spectrum of the Fe-Ar hollow cathode, Ar III 4*s*-4*p* lines identified.

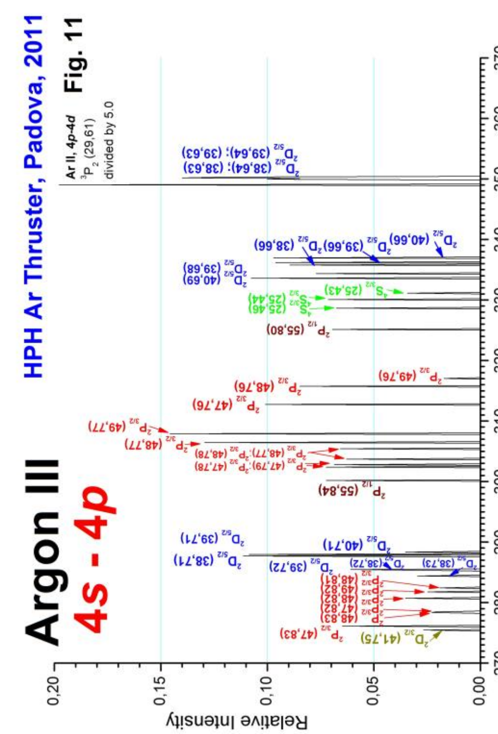

Figure 11. Experimental spectrum of the Ar thruster, Ar III 4*s*-4*p* lines identified.

IV. Discussion of typical spectral features

For plasmas which are more or less near LTE, the patterns of the emitted lines intensities are more similar or dissimilar. When in equilibrium, the plasma emits lines of standard intensities, while when away from equilibrium, a C-R model is necessary in order to foresee the line intensities of the non-LTE plasma spectra and to obtain the line intensity ratios corresponding to each pair of T_e, n_e. Inversely, if the intensity ratios are experimentally known, it is then possible to infer the T_e, n_e values[2]. When the plasma is in LTE, the experimental intensity ratios give directly the A_{ij} which are characteristic constants of each species. Evaluation of the obtained emission spectra are complicated from the fact that each species of the studied plasma (here Ar I, II and III) is in a different status of non-equilibrium. Even within the same species, various configurations may be in different equilibrium states. Moreover, each of the line intensities within a given multiplet may follow more or less the equilibrium values. Comparing the low to high current spectral line intensities shapes of the used hollow cathode, we concluded that they are mostly near equilibrium, as discussed elsewhere[20]. Nevertheless, as we can see in the cases of Figs. 2, 4, 6, 8, 10 presented here, this assumption may be not quite satisfied for some lines. This fact, which could be due occasionally to insufficient resolution or possible saturation, is investigated in the following.

We discuss selected spectra and the obtained results separately for some multiplets belonging in each of the three species of interest. To avoid computational details, we show the differences of the near equilibrium hollow cathode spectra from the non-equilibrium ones obtained from the helicon thruster, keeping in mind that a C-R model was necessary for the detailed evaluation, especially for the latter. In so doing, tables comparing the characteristics of selected levels belonging to the 4*s*, 4*p*, 5*p* configurations of the Ar I (Tables I-V) and to the 4*s*, 4*p*, 4*d* one of the Ar II (Tables VI-IX) are provided herewith; the 4*s*, 4*p* Ar III lines are also commented. Transitions between the chosen configurations provide the most intense lines of the studied spectra.

We give in Tables I to IX some details on line intensity and transition probability ratios concerning selected lines appearing in the presented spectra. These illustrate the fact that the plasma in the thruster is mostly outside LTE, as it can be seen directly from inspection of Figs. 2 to 11. Whenever the plasma is in LTE, at least for some levels of the atomic multiplet, we can determine A_{ij} values and intensity ratios using the well-known simplified formula

$$A_{ij,1} = A_{ij,2} \cdot \frac{I_1}{I_2} \cdot \frac{g_2}{g_1} \cdot \frac{\lambda_1}{\lambda_2} \qquad\qquad \frac{I_1}{I_2} = \frac{A_{ij,1}}{A_{ij,2}} \cdot \frac{g_1}{g_2} \cdot \frac{\lambda_2}{\lambda_1} \tag{2}$$

with the differences of the upper energy levels neglected. g stand for the upper levels statistical weights.

A. Ar I line intensities

A first estimation of the plasma situation can be given by looking to the relative intensities of the Ar I lines.

Fig. 2 shows the main lines of the Ar 4*s*-4*p* multiplet (Ar "red" lines) of the hollow cathode plasma, for low and high current. Intensities of the latter case were divided by a factor for comparison. The corresponding intensities for the helicon plasma case are given in Fig. 3. We see that lines noted 1, 3 and 4 are not in equilibrium, to the contrary of lines 2 which are in equilibrium as are also most of the lines. The corresponding data are given in Table I.

Table I. Description, A_{ij} and intensities of four Ar I 4*s*-4*p* lines, see Figs. 2 and 3.

#	Core	i,j	λNIST	A_{ij}CbA	A_{ij}NIST	IntIΩAlow	IntIΩAhigh	IntPADOVA	g_j
1	2P1/2	5,15	750.387	4.25	4.45	13.	7.2 saturated?	4.9	1
2	2P3/2	3,11	751.465	4.21	4.02	5.9°	5.9°	3.7	1
3	2P3/2	2,10	763.511	2.98	2.45	10.8°	7.4 saturated?	9.5°	5
4	2P3/2	2,7	811.531	3.36	3.31	9.9°	7.6 saturated?	10.7°	7

°:adapted intensities

In Table II we give the ratios obtained after division by the line 2 intensity for two different sets of values:

Table II. Intensity ratios for Table I from theory and experiment.

	Low current	High current	PADOVA	THEORY,LTE*	THEORY,LTE#
I_1/I_2	2.2	1.2 saturated?	1.3	.96	1.05
I_3/I_2	1.8	1.3 saturated?	2.6	3.5	3.0
I_4/I_2	1.7	1.3 saturated?	2.9	5.2	5.3

*using A_{ij} from CbA calculations; #using NIST A_{ij} results

We see that the theoretical LTE values are in agreement, but the experimental values are here away from equilibrium. This is not the case for the Ar I 4*s*-5*p* “blue” lines shown in Figs. 4 and 5 presenting the hollow cathode and the helicon plasmas lines correspondingly. Let us consider the lines 5, which seem to be not quite in equilibrium, with line 6 being mostly in equilibrium. The corresponding data are given in Table III.

Table III. Description, A_{ij} and intensities of two Ar I 4*s*-5*p* lines, see Figs. 4 and 5.

#	Core	i,j	λNIST	A_{ij}NIST	IntIΩAlow	IntIΩAhigh	IntPADV	g_j
5	2P3/2	2,36	415.859	.14	2.9	2.3	2.56	5
6	2P1/2	5,43	425.936	.40	1.36°	1.36°	1.36°	1

°:adapted intensities

In Table IV we give again the ratios obtained by division of the lines 5 and 6 intensities:

Table IV. Description, A_{ij} and intensities of two Ar I 4*s*-5*p* lines, see Figs. 4 and 5.

	Low current	High current	PADOVA	THEORY,LTE#
I_5/I_6	2.1	1.7	1.9	1.8

#using NIST A_{ij} results

Here the experimental values are near the theoretical ones for LTE. The corresponding A_{ij} are given in Table V.

Table V. A_{ij} values for Table III from theory and experiment#.

	NIST	ExpIΩAlow	ExpIΩAhigh	ExpPADOVA
A_{ij}5	.14	.16	.13	.15

#Line 6 A_{ij} values from NIST.

B. Ar II line intensities

In the case of the Ar II species, the 4*s*-4*p* multiplet lines are in the blue plasma region, near the 4*s*-5*p* “blue” lines of the Ar I. This simplifies the comparison of the two species spectral intensities. Fig. 6 shows the main lines of the Ar II 4*s*-4*p* multiplet of the hollow cathode plasma, for low and high current. Intensities of the latter case were divided by a factor for comparison. The corresponding helicon plasma spectrum is given in Fig. 7. Although the low-high current spectra are quite similar, the spectrum in Fig. 7 is quite different from this of Fig. 6. We explain that by the fact that the Ar II spectrum in the thruster is mostly coming from a region around the plasma axis, where the non-equilibrium is expected to be important. Lines of the hollow cathode being rather “off” equilibrium are marked by dots in the Figs. 6 and 7. The lines marked by ¤ in Fig. 6 give about 20% “off” equilibrium.

Next Ar II multiplet of interest is this of the 4*p*-4*d* multiplet. Spectra of the cathode plasma and of the helicon plasma are given in Figs. 8 and 9 correspondingly. Most lines of Fig. 8 are in equilibrium, set aside some cases marked by dots. Data corresponding to the lines marked by 7, 8, 9 are given in the Table VI, analogous to Table I.

Table VI. Description, A_{ij} and intensities of three Ar II 4*p*-4*d* lines, Figs. 8 and 9.

#	Core	i,j	λNIST	A_{ij}CbA	A_{ij}NIST	IntIΩAlow	IntIΩAhigh	IntPADV	g_j
7	3P1	33,68	357.66	25.	28.	.28°	.29°	.33	8.
8	3P2	32,67	358.84	29.	30.	.34°	.35	.33°	10.
9	1D2	52,103	373.79	18.	23.	.19	.27	.17	8.

°:adapted intensities

The intensity ratios of the lines 7 and 9 obtained after dividing by the line 8 intensity are given in Table VII compared to two theoretical results. As it can be seen in the two following Tables VIII and IX, lines 7 and 9 are near LTE because the 4*p*-4*d* multiplet is situated in a higher energy region.

Table VII. Intensity ratios for Table VI from theory and experiment.

	Low current	High current	PADOVA	THEORY,LTE*	THEORY,LTE#
I_7/I_8	.82	.83	1.0	.69	.75
I_9/I_8	.56	.77	.52	.48	.59

*using CbA results, #using NIST A_{ij} results

Table VIII. A_{ij} values for Table VI from theory and experiment#.

	CbA	NIST	ExpIΩAlow	ExpIΩAhigh	ExpPADV
A_{ij}7	25.	28.	30.	30.	36.
A_{ij}9	18.	23.	21.	29.	20.

#Line 8 A_{ij} value from CbA

Table IX. A_{ij} values for Table VI from theory and experiment#.

	CbA	NIST	ExpIΩAlow	ExpIΩAhigh	ExpPADV
A_{ij}7	25.	28.	31.	31.	37.
A_{ij}9	18.	23.	22.	30.	20.

#Line 8 A_{ij} value from NIST

A first estimation of the plasma temperature can be obtained by comparison of the Ar I, Ar II line intensities of the (Ar I) 4*s*-5*p* and (Ar II) 4*s*-4*p* multiplets of the two species. These are seen in Figs. 4 and 5. From our C-R model, we estimated that the relative intensity of those two multiplet lines indicate a temperature of more than 1.5 eV for a n_e of near 10^{12} cm^{-3}. This estimation corresponds to a temperature of the plasma as a whole, following the actual optical path. Nevertheless, this estimation of the plasma T_e and n_e (and accordingly the ionization percentage) encompass big part of the colder plasma situated in the edge region. Therefore, whenever the T_e, n_e are evaluated from the Ar I / Ar II line intensities ratio, the Ar I percentage is overestimated, because the optical line passes from the external cold plasma region, where the abundance of Ar I prevails. Accordingly, the obtained bulk T_e is artificially lowered.

C. Ar III line intensities

Fig. 10 shows the main lines of the Ar III 4*s*-4*p* multiplet of the hollow cathode plasma, for high current. The corresponding helicon plasma spectrum is given in Fig. 11. For the low current spectra of the hollow cathode the 4*s*-4*p* lines were not visible, because the available energy was not sufficient.

Comparing the two spectra we can easily infer for the helicon plasma that temperature of the Ar III species, which are in principle more abundant near the axis, is higher than in the bulk of the hollow cathode.

Using the Ar II / Ar III ratio we can achieve a better evaluation of the T_e in the plasma core. Indeed, the so obtained T_e concerns essentially the central part of the plasma, where the essential part of the Ar II and Ar III amount is concentrated. Focusing at the same time in the Ar II and Ar III lines, which span the 200 nm to 500 nm region, we can determine the temperature from the intensity ratios mostly in the central region.

From our C-R model, for a n_e of 10^{12} cm^{-3} the Ar III lines are expected to appear at about 1.9 eV. Whenever they are visible, we obtain a minimal estimation of the core region temperature. The most intense lines of Ar III belong to the 4*s*-4*p* multiplet and they are notably appearing in the region from 320 nm to 355 nm (see Figs. 10 and 11).

The Ar III 4*p*-4*d* lines (mainly from 200 to 300 nm) can also be clearly seen when the temperature

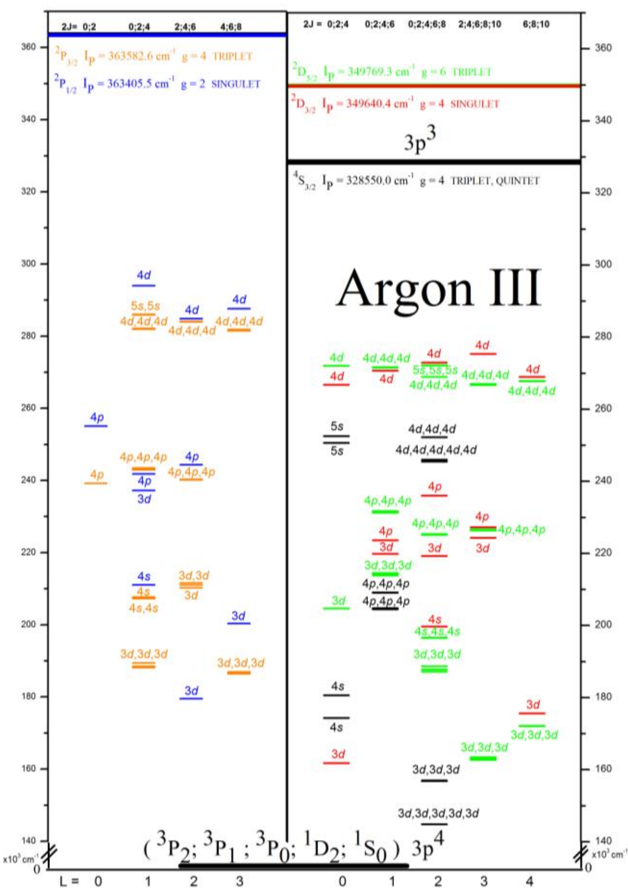

Figure 12. Grotrian diagram of Ar III.

exceeds 2.5 eV. This temperature difference (from 1.9 eV to 2.5 eV) is due to the energy gap between the 4*p* and 4*d* levels, as can be seen by inspection of the Ar III Grotrian diagram given in Fig 12. As we have observed the more intense lines of the 4*p*-4*d* multiplet, we may infer that this is the case for the helicon plasma, for which our C-R calculations are giving a T_e exceeding 3 eV for n_e about 10^{12} cm^{-3}. It is also to take into consideration that the measurements inside the thruster have been made through a Pyrex glass, which was measured to substantially absorb in the shorter wavelength region. When this selective absorption was taken into account, the obtained T_e values have been found to be at least 25 % higher, which resulted also to a slight increase of the corresponding n_e values (of about 10 %) estimated from the 4*p*-4*d* multiplet lines intensities. Actually, the effective T_e values could be proved to be higher, as the present optical part of the experimental set-up in the 200 nm – 300 nm wavelength region is not sufficient to allow for assessment of any higher T_e values. In fact, to insure diagnosing of higher T_e values, additional identification of lines belonging to other multiplets is required. In so doing, acquisition of VUV spectra could be very helpful in this context, as discussed elsewhere[19].

V. Conclusion

OES was successfully applied in diagnosing a helicon plasma thruster. In so doing, previous emission spectra measurements and a C-R model have been extensively used.

Acknowledgment

The research leading to these results has received funding from the European Community's Seventh Framework Programme (FP7/2007-2013) under grant agreement n° 218862.

References

[1] Boffard J.B., Jung R.O., Lin C.C., Wendt A.E., *Optical Emission Measurements of Electron Energy Distributions in Low-pressure Argon Inductively Coupled Plasmas*, Plasma Sources Sci. Technol. **19** 065001, 2010.

[2] Katsonis K., Pellerin S., Dzierzega K., *C-R type Modeling and Application in Plasma Diagnostics*, JHTMP **7** 559, 2003.

[3] Katsonis K., Siskos A., Dzierzega K., Pellerin S., Tanguy M., *C-R Modeling of Ar Plasmas: Low Temperature Validation*, in ESA SP-555, A.Wilson Edtr., 4th ISPC, p. 129.1, 2-9 June 2004, Sardinia (Italy).

[4] Pavarin D., Ferri F., Manente M., Cuirreli D., Güçlü Y., Melazzi D., Rondini D., Suman S., Carlsson J., Bramanti C., Ahedo E., Lancellotti V., Katsonis K., Markelov G., *Design of 50 W Helicon Plasma Thruster*, IEPC-2009-**205**, 31th IEPC Conference, Sept. 2009, Ann Arbor, MI, USA

[5] Pavarin D. , Ferri F., Manente M., Rondini D., Curreli D., Guclu Y., Melazzi D., Suman S., Bianchini G., Packan D., Elias P., Bonnet J., Tuccillo A., Deangelis R., Tudisco O., Mirizzi F., Cardinali A., Ahedo E., Protsan Y., Loyan A., Piergentili F., Grue K., van Put P., Selmo A., Katsonis K., Pessana M., Carlsson J., *Helicon Plasma Hydrazine.Combined Micro Project Overview and Development Status*, Space Propulsion SP2010 Conference, 3-6 May 2010, San Sebastian, Spain

[6] Monahan D.D., Turner M.M., *Global Models of Electronegative Discharges: Critical Evaluation and Practical Recommendations*, Plasma Sources Sci. Technol. **17** 045003, 2008

[7] K. Katsonis, Ch. Berenguer, Collisional-Radiative Modeling for Diagnostics and Modeling of Plasma Thrusters, Space Propulsion SP2010 Conference, 3-6 May 2010, San Sebastian, Spain

[8] Pavarin D., Ferri F., Manente M., Lucca Fabris A., Faenza M., Trezzolani F., Tasinato L., Tudisco O., Loyan A., Protsan Y., Tsaglov A., Selmo A., Katsonis K., Berenguer Ch, Packan D., Jarrige J., Blanchard C., Elias P.Q., Bonnet J., *Thruster Development Set-up for the Helicon Plasma Hydrazine Combined Micro Research Project*, IEPC-2011-**241**, 32th IEPC Conference, Sept. 2011, Wiesbaden, Germany

[9] Katsonis K., Clark R.E.H., Cornille M., Berenguer Ch., Humbert D., Ndiaye A., Maynard G., *Atomic Data for Fusion Reactor Impurities*, ECAMP IX Conference, 7-11 May 2007, Creta, Greece.

[10] Katsonis K., Bonnet J., Packan D., Berenguer Ch., Cornille M., Ndiaye A., *Field Emission Electric Thruster Optical Diagnostics Based on an Indium Collisional-Radiative Model*, IEPC-2007-**284**, 30th IEPC07 Conference, 17-20 September 2007, Florence, Italy.

[11] Lieberman M.A., Lichtenberg A.J., *Principles of Plasma Discharges and Materials Processing*, 2d Ed., J. Wiley and sons, Hoboken, NJ, 2005

[12] Gordillo-Vàzquez F.J., Camero M., Gomez-Aleixandre C., *Spectroscopic Measurements of the Electron Temperature in Low Pressure Radiofrequency Ar/H_2/C_2H_2 and Ar/H_2/CH_4 Plasmas Used for the Synthesis of Nano-carbon Structures*, Plasma Sources Sci.Technol. **15** 42, 2006

[13] Boffard J.B., Jung R.O., Lin C.C., Wendt A., *Measurement of Metastable and Resonance Level Densities in Rare Gas Plasmas by Optical Emission Spectroscopy*, Plasma Sources Sci. Technol. **18** 035017, 2009

[14] Berenguer Ch., Katsonis K., Danakas S., Cohen S., Tsekeris P., Cornille M., *Study of the First Three Ar I, II, III Spectra Using a C-R Model*, ICAMDATA 06 Conference, 28-31 October 2008, Beijing, China

[15] Katsonis K., Otte M., Krychowiak M., Tsekeris P., Berenguer Ch., Cohen S., *Optical Diagnostics on WEGA Stellarator using Ar and Xe C-R Models*, EGAS41 Conference, 8-11 July 2009, Gdansk, Poland
[16] Berenguer Ch., *Optical Diagnostics of High Energy Density Plasmas*, PhD Thesis, Orsay, February 2009
[17] Katsonis K., Berenguer Ch., Kaminska A., Dudeck M., *Argon 4s and 4p Excited States Atomic Data Applied in Arc-Jet Modeling*, IJAE, 2011 (in press)
[18] Katsonis K., Berenguer Ch., Cornille M., *A Simple Atomic Scheme for Ar Thruster Multidimensional Modeling and Optical Diagnostics*, IEPC-2009-**035**, 31th IEPC Conference, Sept. 2009, Ann Arbor, MI, USA
[19] Berenguer Ch., Katsonis K., Pavarin D., *The Resonant Lines VUV Transitions in Rare Gas Plasma Thrusters*, IEPC-2011-**170**, 32th IEPC Conference, Sept. 2011, Wiesbaden, Germany
[20] Berenguer Ch., Katsonis K., Tsekeris P., Cohen S., Cornille M., Clark R.E.H., *Measurement and Evaluation of Transitions Probabilities of Ar I to III*, EGAS43 Conference, July 2011, Fribourg, Switzerland
[21] Lafleur T., Charles C., Boswell R.W., *Characterization of a Helicon Plasma Source in Low Diverging Magnetic Fields*, J. Phys. D **44**, 2011
[22] Batitschev O.V., *Minihelicon Plasma Thruster*, IEEE **37** 1563, 2009
[23] Katsonis K., Drawin H.-W., *Transition Probabilities for Ar(I)*, JQSRT **23** 1, 1980.
[24] Eissner W., Jones M., Nussbaumer H., *Techniques for the Calculation of Atomic Structures and Radiative Data Including Relativistic Corrections*, Com. Phys. Comm. **8** 270, 1974
[25] Abdallah Jr. J., Clark R.E.H., Cowan R.D., *CATS: The Cowan Atomic Structure Code*, Report LA-11436-M, 1988, Los Alamos, USA. / URL http://aphysics2.lanl.gov/tempweb/
[26] Ralchenko Yu., Kramida A.E., Reader J., NIST ASD Team 2010, NIST Atomic Spectra Database (version 3.1.5), National Institute of Standards and Technology, Gaithersburg, MD, USA / URL http://physics.nist.gov/PhysRefData/ASD/index.html